Eur. Phys. J. B **32**, 339–344 (2003)
DOI: 10.1140/epjb/e2003-00107-6

THE EUROPEAN PHYSICAL JOURNAL B

Effects of the indium doping on structural and optical properties of CdSe thin films deposited by laser ablation technique

G. Perna[1,2,a], V. Capozzi[1,2], A. Minafra[2,3], M. Pallara[4], and M. Ambrico[5]

[1] Facoltà di Medicina e Chirurgia dell'Università di Foggia, Viale L. Pinto, 71100 Foggia, Italy
[2] Istituto Nazionale di Fisica della Materia, Unità di Bari, Via Amendola 173, 70126 Bari, Italy
[3] Dipartimento Interateneo di Fisica dell'Università di Bari, Via Amendola 173, 70126 Bari, Italy
[4] Dipartimento Geomineralogico dell'Università di Bari, Via Amendola 173, 70126 Bari, Italy
[5] Istituto di Metodologie Inorganiche e dei Plasmi del C.N.R., Via Orabona 4, 70126 Bari, Italy

Received 27 September 2002
Published online 11 April 2003 – © EDP Sciences, Società Italiana di Fisica, Springer-Verlag 2003

Abstract. Thin films of n-type CdSe have been grown on a quartz substrate by laser ablating a target obtained by mixing CdSe and metallic In powders. The effects of different doping concentration of In have been investigated. X-ray diffraction spectra show that at low In density only the CdSe lattice is present in the deposited film, whereas $CdIn_2Se_4$ and InSe compounds are deposited at higher In concentration. Band gap narrowing and band tails are observed in the absorption spectra when the In concentration increases. Photoluminescence spectra show band-band recombinations from 10 K to room temperature.

PACS. 78.40.Fy Semiconductors – 78.55.Et II-VI semiconductors

1 Introduction

Thin films of II-VI semiconductors are of considerable interest for their excellent optical properties in the visible range. In particular, CdSe compounds have become quite interesting for solar cells, photodetection and optoelectronic applications [1]. The electronic and optical properties of semiconductors are strongly influenced by the doping process, which provides the basis for tailoring the desired carrier concentration and, consequently, the absorption, emission and transport properties as well. In fact, the increase of the doping density causes the broadening of the intragap impurity bands. In particular, when the density of n-type or p-type doping becomes sufficiently high, the impurity band merges with the conduction or valence band and causes the formation of a band tail [2] and band gap shrinkage [3].

In this work, we mainly discuss experimental data for n-doped CdSe. To take advantage of the many attractive optoelectronic properties of CdSe, extrinsic doping techniques to produce (controlled) n-type doping are required. A typical dopant used to obtain n-type CdSe is indium (In), a cation site dopant: in fact, substituting Cd in CdSe, indium acts as a donor. Different methods exist to obtain In doped CdSe thin films: solution growth [1], co-evaporation method [4], chemical bath and electrodeposition [5]. We have deposited In doped CdSe thin films at different In concentrations, by means of the pulsed laser ablation technique. These films show a crystalline quality, as deduced from X-ray diffraction (XRD) measurements. Optical characterization has been carried out by absorption and photoluminescence (PL) measurements. A red shift of the absorption edge and band-band luminescence have been observed when the indium concentration increases: this effect is consistent with a merging of the donor band with the conduction band when the indium concentration become sufficiently high.

[a] e-mail: giuseppe.perna@ba.infn.it

2 Experimental

Indium doped CdSe thin films have been deposited by laser ablating stoichiometric home-made targets, obtained by properly mixing and cold pressing high purity (99.999%) powders of CdSe and metallic indium powder. Our method is quite different from that used by Park *et al.* [6] to obtain In doped CdSe films with the laser ablation technique: in fact, they obtained the In doping by attaching an indium wire to the CdSe target and bonding the GaAs substrate to the base plate by means of indium. Our films were deposited on an amorphous quartz substrate, in order to perform transmission measurements around the absorption edge region of CdSe. In particular, we fixed the In powder weight to 1%, 5% and 10% of the CdSe powder weight, so obtaining three CdSe:In films with different doping density. A pulsed Nd:Yag laser

operating at 532 nm was used as the laser source, with a pulse duration of about 10 ns and a repetition rate of 10 Hz. The laser fluence and substrate temperature were optimized to about 10 J/cm^2 and 400 °C, respectively. The deposition chamber was evacuated to a residual pressure of about 10^{-6} mbar before starting the deposition process. The substrate was mounted on a rotating support at a distance of 3 cm from the target. The thickness of the films, as measured from an alphastep profilometer, was found to be about 0.5 μm for the CdSe: In(1%) and about 0.3 μm for the CdSe: In(5%) and CdSe: In(10%) films.

XRD analysis was performed by using the CuKα radiation (γ = 1.5406 Å) of a $\theta - 2\theta$ diffractometer. Spectra of the absorption coefficient (α) were obtained from the Lambert-Beer law $\alpha = (1/d)\exp(1/T)$, where d is the film thickness and T is the film transmittance, measured by employing a 100 W tungsten lamp light source. The reflectance contribution to the α value has been neglected because the reflectance values of CdSe films are much lower than the transmittance ones in the examined spectral region. Moreover, the quartz substrate is transparent in the investigated spectral region: therefore, it weakly influences the optical measurements. The samples were mounted in a He-closed cycle refrigerator thermoregulated from 10 to 300 K. The light transmitted from the sample was analysed by means of a double grating spectrometer (1 meV/mm of dispersion) and detected by a GaAs:Cs (cooled to –20 °C) photomultiplier, using the photon counting technique. For the PL measurements, the line 458 nm of an Ar ion laser was used for excitation. Standard backscattering geometry for PL was used. The PL light emitted from the sample surface was analysed and detected by the same spectrometer and photomultiplier used for the transmittance measurements.

3 Results and discussion

3.1 XRD measurements

The XRD spectra at room temperature of the three CdSe:In deposited films are shown in Figures 1a, b, c. A XRD spectrum of an undoped CdSe films deposited on a silicon substrate with the laser ablation technique (Fig. 1d) is also shown for comparison purposes. The peak at about 25.4° refers to the (002) reflection of the CdSe lattice: this suggests that the films grow according to a preferential orientation of the hexagonal phase. However, other diffraction peaks are visible in the XRD spectra of the CdSe: In(5%) and CdSe: In(10%) films. In particular, the peak at 26.4° (Figs. 1a and 1b) refers to the (111) orientation of the tetragonal phase of the $CdIn_2Se_4$ and the small structure at 21.3° (Fig. 1c) refers to the (400) orientation of the hexagonal phase of InSe. Therefore, the XRD spectra indicate that at low In concentration only the CdSe compound is present, whereas the increase of the In concentration causes also the formation of the $CdIn_2Se_4$ (at medium In concentration) and InSe compounds (at larger In concentration). We deduce

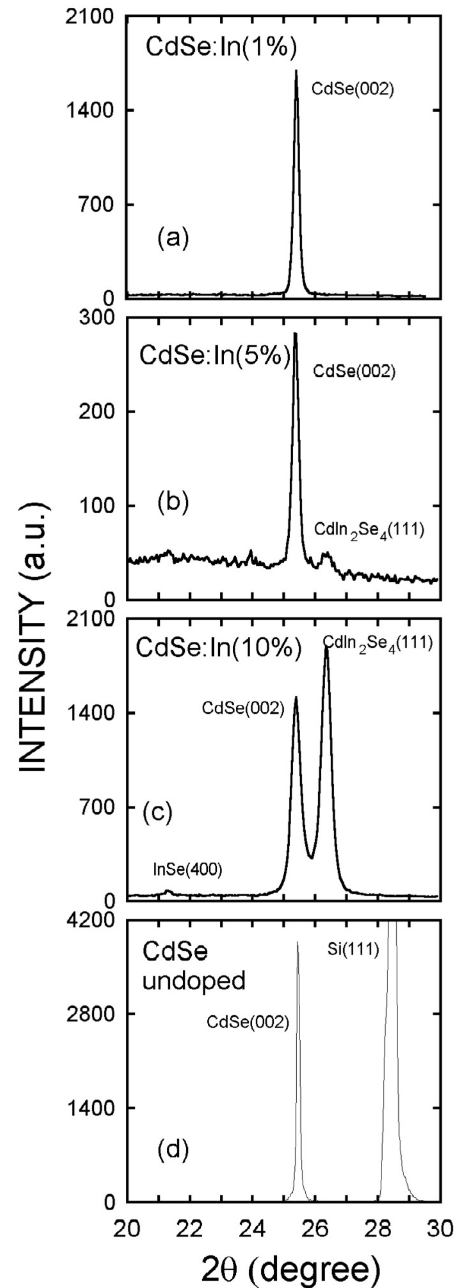

Fig. 1. XRD spectra of three CdSe:In samples deposited on a quartz substrate with different In concentrations: (a) 1%, (b) 5%, (c) 10%. The Miller indexes of the reflection from the CdSe, $CdIn_2Se_4$ and InSe compounds are indicated. The XRD spectrum of an undoped CdSe film deposited on a silicon substrate by the laser ablation technique (reprinted from [9]) is shown in Figure 1d for comparison purposes.

that the deposition technique is only suitable for growing CdSe:In thin films when the In concentration is lower than a few percent. Therefore, in what follows we shall discuss the electrical and optical data referring to CdSe: In(1%) and CdSe:In(5%). Moreover, the increase of the In content causes a broadening of the CdSe (002) peak, corresponding to a decrease of the average grain size, D, of the

films. In fact, an estimate of the D values according to the Debye-Schrerrer relationship [7], gives $D = 44.7 \pm 0.5$ nm, $D = 38.2 \pm 0.3$ nm and $D = 23.6 \pm 0.3$ nm for CdSe: In(1%), CdSe: In(5%) and CdSe: In(10%), respectively. These D values should be compared with the corresponding values obtained for undoped CdSe films deposited on different substrates. The average grain size estimated for undoped CdSe deposited on quartz, $D = 42.6$ nm [8], is comparable with that of the CdSe: In(1%) and CdSe: In(5%), so indicating the good structural properties of our n-doped CdSe films. In fact, the CdSe lattice is not dramatically influenced by the high density of In atoms. In contrast, the structural properties of the films strongly depend on the deposition substrate: the XRD peak of the CdSe film deposited on silicon is much narrower than the corresponding peak of the CdSe film deposited on quartz, as is visible in Figure 1. In fact, the average grain size estimated for CdSe films deposited on a crystalline Si (111)-oriented substrate, $D = 100$ nm [9] is much larger than that of CdSe films deposited on quartz.

The n-type doping in the CdSe:In(1%) and CdSe:In(5%) films has been confirmed by means of Hall effect measurements at room temperature. The electron carrier concentration was estimated to be $\sim 1.3 \times 10^{21}$ cm^{-3} and $\sim 9.7 \times 10^{21}$ cm^{-3} in CdSe: In(1%) and CdSe: In(5%) films, respectively. This enhancement in carrier concentration value is responsible for the observed decrease of the electric resistivity with the rise in In doping density: in fact, values of about 0.34×10^{-4} ohm cm^{-1} and 0.14×10^{-4} ohm cm^{-1} have been found for CdSe: In(1%) and CdSe: In(5%), respectively. On the other hand, the mobility value decreases with increasing In concentration: in fact, values of 146 cm^{-2} V^{-1} s^{-1} and 45.2 cm^{-2} V^{-1} s^{-1} have been found for CdSe:In(1%) and CdSe:In(5%), respectively. This effect can be due to the increase of impurity and defect scattering with increasing In content.

3.2 Absorption measurements

A large amount of dopants induces a large free carrier density in the bands and a high density of ionized dopant ions: these facts cause a variation in the density of states with respect to the undoped case and the formation of band tails, which strongly influence the optical properties. In defect-free crystalline semiconductors, the conduction and valence band distributions of states terminate abruptly at their respective band edge; therefore, an energy gap is clearly defined for such materials. In contrast, the presence of tail states in highly doped semiconductors make it difficult to give a realistic energy gap value for these materials. Several experimental methods enabling an estimate to be made of the energy gap value for these materials have been developed [10]. The most common methods are based on absorption measurements. The estimate of the energy gap value obtained by means of absorption measurements is known as "optical gap". One of the standard empirical methods to obtain the optical gap value is the

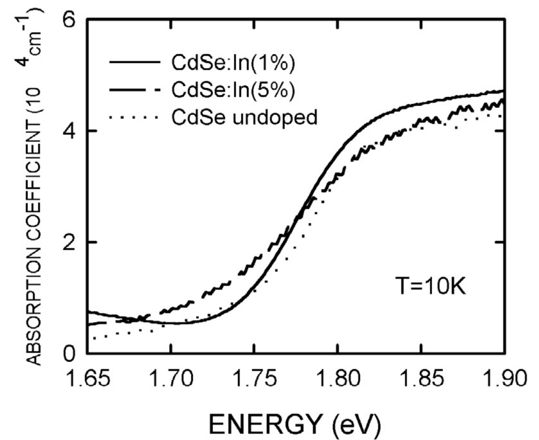

Fig. 2. Absorption coefficient of CdSe:In(1%) (continuous line) and CdSe:In(5%) (dashed line) films deposited on a quartz substrate, measured at 10 K in the near band gap region. The absorption coefficient is calculated by the Lambert-Beer law (see text). The absorption coefficient of an undoped CdSe film is also reported for comparison purposes.

Tauc method [11], which was originally related to amorphous materials: in this model, the optical gap Eg_{opt} value in the strong absorption region ($\alpha > 10^4$cm^{-1}) is defined according to:

$$\alpha(h\nu)h\nu = A(h\nu - Eg_{opt})^r \quad (1)$$

where h is the Planck constant, A is a constant and r is a number which characterizes the transition process: r has a value of 1/2 for the direct allowed transition. The above relationship is exactly valid for parabolic conduction and valence bands near the band gap.

A decrease of the optical band gap and broadening of the absorption edge result when the doping density increases. Such effects are clearly evident in Figure 2, where the spectrum of the absorption coefficient α near the absorption edge at $T = 10$ K is shown for the CdSe:In(1%) and CdSe:In(5%) films. The absorption spectrum of an undoped CdSe film deposited on a quartz substrate by laser ablation is also shown for comparison purposes. As can be seen in Figure 2, discrete excitonic features are absent in both the doped and undoped films. This is due to two combined effects: i) the structural disorder induced by the lattice mismatch between the quartz substrate and the CdSe film causes local electric fields which dissociate the excitons; ii) the increase of the free carriers with doping density enhances the electric screening between holes and electrons and reduces the intensity of the oscillator strength of the discrete exciton states. Therefore, the absorption edge of the CdSe films in Figure 2 is characterized by continuum state transitions.

Besides the doping density, the lattice temperature influences the spectral position of the optical band gap. The absorption spectra of the CdSe:In(1%) and CdSe:In(5%) films at different temperatures are reported in Figures 3a and b, respectively. The absorption spectrum of each film shifts to lower energy as the temperature increases: this effect, which is well known for undoped semiconductors,

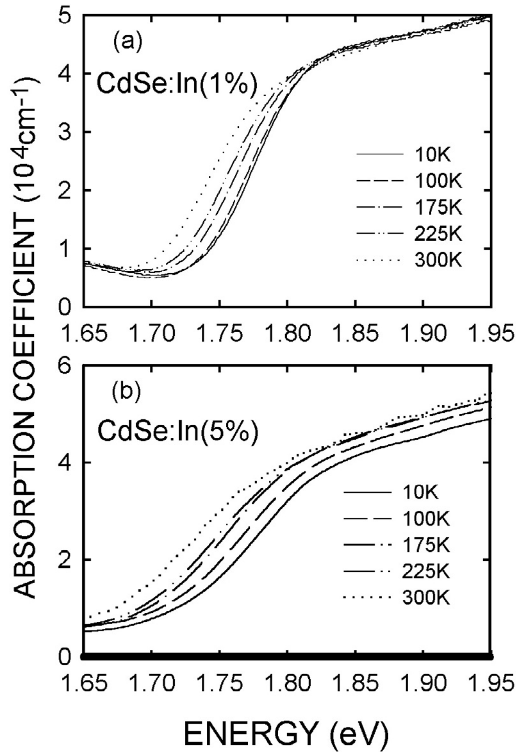

Fig. 3. Absorption coefficient of CdSe:In(1text).

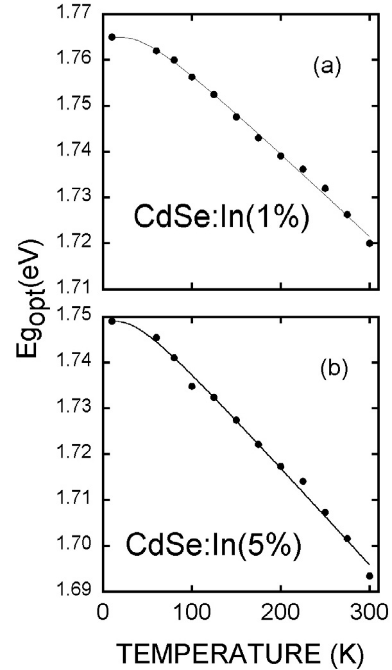

Fig. 4. Temperature dependence of the optical gap (dots) of the CdSe:In(1%) (a) and CdSe:In(5%) samples, obtained from Figure 3. The continuous lines are the best fits to equation (2).

is due to the thermal expansion of the film lattice and the temperature dependence of the electron-phonon interaction [12]. An estimate of the Eg_{opt} values at different temperatures has been deduced by applying the Tauc method [11]. However, this method, which is based on a linear extrapolation to the energy axis of the $(\alpha h\nu)^2$ *versus* $h\nu$ (according to Eq. (1) for $r = 1/2$), is an empirical method which underestimates the band gap value. In fact, O'Leary *et al.* [13] demonstrated that the Tauc gap overestimates the broadening of the absorption spectrum. As a consequence, the optical gap deduced from the Tauc method is lower than the effective one. So, the obtained Eg_{opt} values can be considered to be only an approximate estimate of the absorption edge. The Eg_{opt} values at different temperatures are reported in Figures 4a and b (dots) for CdSe:In(1%) and CdSe:In(5%) films, respectively.

The thermal shrinkage of the optical gap can be described by the empirical model introduced by Viña *et al.* [12]:

$$Eg_{opt}(T) = Eg_{opt} - 2a_B n_B \quad (2)$$

where a_B is the strength of the electron-phonon interaction, $n_B = [\exp(\theta/T) - 1]^{-1}$ is the Bose-Einstein statistical factor for phonon emission and absorption, θ is a temperature corresponding to an average energy for the phonons involved in the process. This model (the continuous lines in Fig. 4) fits well the Eg_{opt}(T) data of both samples. The parameters obtained by the fitting procedure give information about the electron-phonon interaction in the films. The θ value indicates how large the contribution is of acoustic phonons to the red-shift of the optical gap: the lower the θ value with respect to the longitudinal optical (LO) phonon temperature, the larger the contribution of acoustic phonons to the optical gap shrinkage due to electron-phonon interaction. In particular, the values of the parameter $\theta = 143 \pm 12$ K and $\theta = 126 \pm 10$ K obtained for CdSe:In(1%) and CdSe:In(5%), respectively, indicate that acoustic as well as optical phonons contribute to the optical gap shrinkage. Indeed, the LO phonon energy corresponds to a temperature of about 300 K for CdSe [14], well above the average θ value obtained by our fitting for the two doped compounds. These θ values should be compared with the θ values obtained by analysing the temperature dependence of the band gap for undoped CdSe deposited on amorphous quartz ($\theta = 189 \pm 10$ [15]) and crystalline silicon (111)-oriented substrate ($\theta = 201 \pm 3$ [9]). It can be deduced that the contribution of acoustic phonons to the band gap shrinkage increases with the structural disorder. In fact, the θ value is larger for the films deposited on a crystalline substrate and it decreases when the deposition occurs on an amorphous substrate. In addition, the θ value decreases with increasing the doping density of the films. Such a behaviour suggests a correlation between the structural disorder (which increases with the doping density, especially if the deposition occurs on amorphous substrates) and the damping of the optical phonons [9].

Moreover, the fitting procedure permits an evaluation of the $Eg_{opt}(0)$ values, *i.e.* the limiting value of the optical gap at low temperature: the result is about 1.765 eV for CdSe:In(1%) and 1.749 eV for CdSe:In(5%). These values are well below the values reported in the literature for the energy gap of CdSe single crystals (1.840 eV at $T = 2$ K [14]) and undoped CdSe films deposited on quartz

substrate (1.814 eV at $T = 10$ K [15]). The effects of band gap shrinkage have been extensively studied both theoretically and experimentally for several semiconductors [16,17]. In addition, the difference between the optical gap of the two doped CdSe films, which is about 16 meV at low temperature, increases with temperature to around 26 meV at 300 K. This behaviour is probably due to an overestimated contribution of the broadening of the absorption tail (which increases with the temperature) to the evaluation of the optical gap value, as explained before.

3.3 Photoluminescence measurements

The effects of doping strongly influence also the PL properties of a semiconductor. In fact, this technique, which measures the spectrum emitted by the radiative recombinations of photogenerated minority carriers, is a direct way to measure the band gap energy. However, a large amount of impurities induces a large free carrier density in the bands and a high density of ionized dopant atoms as well. Consequently, different carrier interactions cause remarkable modifications of the lineshape and spectral energy of the PL features. First of all, when the doping density is sufficiently high the disorder due to stoichiometric fluctuations generates strong local fields which dissociate the exciton bound states: therefore, only electron-hole recombinations (band-band emission) characterizes the PL spectrum in the band edge region. In addition, strains due to lattice mismatch and thermal expansion differences between substrate and films contribute to the structural disorder and cause a broadening of the emission band and the decrease of the luminescence intensity because of the introduction of non radiative recombination centres. Furthermore, renormalization of the band gap occurs when impurity tails merge into the conduction or valence band: this causes a red- shift and broadening of the PL features.

These effects are evident in the PL spectra of the CdSe:In(1%) and CdSe:In(5%) samples at 10 K, shown in Figure 5. In fact, no excitonic emission is evident but the spectra are characterized by three PL bands. The total PL intensity decreases as the In concentration increases (see the sensitivity scale factors in Fig. 5), because of the increase of non radiative traps and defect centres due to structural disorder. The three PL bands are centred at about 1.79 eV (high energy band), 1.64 eV (medium energy band), 1.43 eV (low energy band) in CdSe:In (1%) and 1.77 eV, 1.61 eV, 1.44 eV in CdSe:In(5%). The energy shift of the PL bands in the two samples are due to the different band gap values.

An attribution of the radiative bands in the three samples can be performed by means of PL measurements as a function of temperature, which are reported in Figures 6a and b for CdSe:In(1%) and CdSe:In(5%), respectively. The higher energy band, persisting from low to high temperature values, is due to band-band emission. This band presents a red-shift with increasing temperature, due to thermal shrinkage of the energy gap. The energy of this band maximum is higher than the energy of the optical gap as deduced from absorption measurements. This is

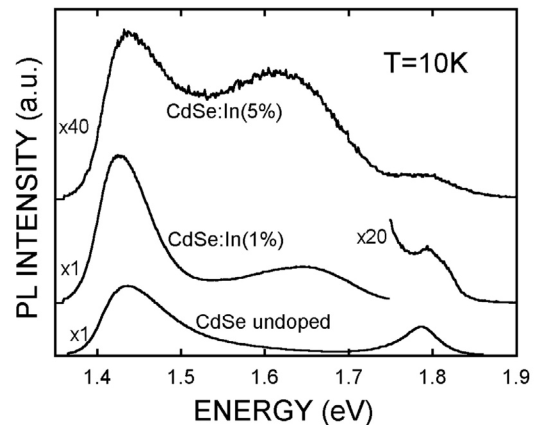

Fig. 5. Photoluminescence spectra of CdSe:In(1%) and CdSe:In(5%) films deposited on a quartz substrate, measured at 10 K. The photoluminescence spectrum of an undoped CdSe film is also shown for comparison purposes. The spectral resolution is 1 meV.

a further confirmation that the Tauc method underestimates the absorption edge value. In fact, by comparing the experimental absorption and PL spectra at $T = 10$ K, in Figures 2 and 5, respectively, it is evident that the intrinsic emission energy is approximately in the same spectral region as the absorption spectra. However, in highly doped semiconductors, besides the mentioned band gap shrinkage due to the doping band tails, the Burstein-Moss effect is also present due to the carrier band filling [16,17]. If we take into account that in our In doped samples a carrier density of the order of 10^{21} cm^{-3} is present, we think that in the intrinsic PL spectra both effects can coexist and cannot be easily distinguished. The spectral position of the maximum of the intrinsic PL band depends on the thermal distribution of the free carriers in the respective conduction and valence band [18].

The PL band at medium energy corresponds to radiative recombinations involving shallow levels in the band gap due to native impurities: in fact, it disappears at a sufficiently high temperature (above 100 K) due to thermal ionization of the involved impurity levels. On the other hand, the low energy band is due to radiative recombinations involving deep impurity levels: indeed, these levels cannot be thermally ionized and the radiative recombinations persist up to room temperature.

4 Conclusion

In conclusion, In doped CdSe thin films have been deposited using the pulsed laser ablation technique, starting from home-made doped CdSe pellets containing an appropriate In weight fraction. Investigation of the structural properties of the deposited films shows that our deposition technique works only when the dopant concentration is not excessively large (lower than a few percent in weight of In). In fact, for small In concentrations (In powder weight up to 5% with respect to the CdSe powder weight

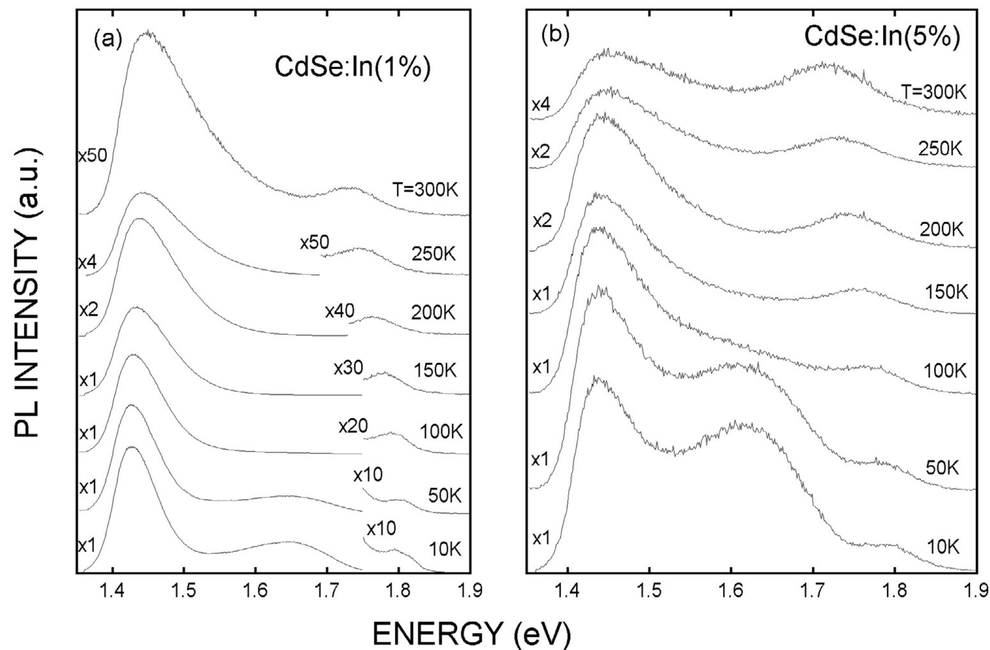

Fig. 6. PL spectra of CdSe:In(1%) (a) and CdSe:In(5%) (b) films, as in Figure 5, measured at different temperatures. The spectral resolution is 1 meV.

in the ablated target) the films grow highly oriented in the hexagonal phase. The absorption spectra are strongly influenced by the heavy doping: in fact, band gap narrowing occurs with increasing doping density. Moreover, it is worth noting that the intrinsic (band-band) luminescence of each film persists at room temperature, as usually occurs for single crystals. This is a promising result for potential optoelectronic applications of laser ablation for easily depositing high doped semiconductor films.

The authors are grateful to A. Cola for the electric measurements and to D. Lojacono for the technical assistance.

References

1. K.C. Sharma, R. Sharma, J.C. Garg, Jpn J. Appl. Phys. **31**, 742 (1992) and references therein
2. E.O. Kane, Phys. Rev. **131**, 79 (1969)
3. A. Haufe, R. Schwabe, H. Fieseler, M. Ilegems, J. Phys. C **21**, 2951 (1988)
4. T. Hayashi, R. Saeki, T. Suzuki, M. Fukaya, Y. Ema, J. Appl. Phys. **68**, 5719 (1990)
5. O. Savagodo, Solar En. Mat. Solar Cells **52**, 361 (1998)
6. J.W. Park, C.M. Rouleau, D.H. Loundes, J. Cryst. Growth **193**, 516 (1998)
7. H.P. Klug, L.E. Alexander: *X-Ray Diffraction Procedures* (Wiley, New York 1954)
8. G. Perna, S. Pagliara, V. Capozzi, M. Ambrico, T. Ligonzo, Thin Solid Films **349**, 220 (1999)
9. G. Perna, V. Capozzi, M. Ambrico, J. Appl. Phys. **83**, 3337 (1998)
10. D.E. Sweenor, S.K. O'Leary, B.E. Foutz, Solid State Commun. **110**, 281 (1999)
11. J. Tauc, R. Grigorovici, A. Vancu, Phys. Status Solidi A **15**, 627 (1966)
12. L. Viña, S. Logothetidis, M. Cardona, Phys. Rev. B **30**, 1979 (1984)
13. S.K. O'Leary, P.K. Lin, Solid State Commun. **104**, 17 (1997)
14. *Landolt-Boernstein Tables*, edited by O. Madelung, M. Schulz, H. Weiss, Vols. 17a and b (Springer, Berlin, 1982)
15. G. Perna, V. Capozzi, S. Pagliara, M. Ambrico, *Proceedings of SPIE* **4070**, 372 (2000)
16. L. Viña, M. Cardona, Phys. Rev. B **29**, 6739 (1984)
17. L. Viña, M. Cardona, Phys. Rev. B **34**, 2586 (1986)
18. L. Pavesi, M. Guzzi, J. Appl. Phys. **75**, 4779 (1994)